

Plug-and-Play Control—Modifying Control Systems Online

Jan Bendtsen, *Member, IEEE*, Klaus Trangbaek, and Jakob Stoustrup, *Senior Member, IEEE*

Abstract—Often, when new sensor or actuator hardware becomes available for use in a control system, it is desirable to retain the existing control system and apply the new control capabilities in a gradual fashion rather than decommissioning the entire existing system and replacing it with an altogether new control system. However, this requires that the existing controller remains in action, and the new control law component is *added* to the existing system. This paper formally introduces the concept of *Plug-and-Play control* and proposes two different methods of introducing new control components in a smooth manner, providing stability guarantees during the transition phase as well as retaining the original control structure. The applicability of the methods is illustrated on two different practical example systems, a livestock stable climate control system and a laboratory-scale model of a district heating system.

Index Terms—Observer-based control, variable structure systems, Youla-Kucera parameterization.

I. INTRODUCTION

ALL medium- to large-scale automation systems, such as power plants, refineries, factories, supermarkets or even large ships, are equipped with control systems to handle various automated processes, such as production facilities [1], [2], chemical batch processing [3], climate control [4], or power production [5]. Most practical control systems tend to be designed at the time of commissioning of the plant and quite often rely on programmable logic controllers (PLCs) or similar hardware to implement classically designed (and often conservatively tuned) control loops. However, as time goes by and new technology and knowledge becomes available, it may become desirable to introduce new sensor and/or actuator hardware for performance reasons.

The problem here is that a vast majority of control design methodologies are “monolithic” in the sense that they embark from a full-scale model of an uncontrolled (open-loop) system and outputs a full, multi-variable control system, which does not exploit any knowledge or functionality from previous designs. If components or sub-systems are added to existing systems, however, the design in principle has to be re-done from

scratch, which is likely to be very expensive in terms of engineering man-hours, operation stop, and commissioning of the new system.

Thus, when new sensor and/or actuator hardware becomes available for use in a control system, it is often desirable to retain the existing control laws and apply the new control capabilities in a gradual, online fashion rather than decommissioning the entire existing control system and replacing it with the new system [6]–[8].

Furthermore, from an industrial application-oriented point of view, the ability to switch back to an existing, proven control design in case a new, more complex design proves unsatisfactory in practical operation, for instance if uncertainties, nonlinear effects or similar causes the performance to degrade, is a significant advantage. In many cases there may also be other arguments for maintaining the existing control system in place, such as it being part of a safety-critical interlocking circuit.

We hereby define the concept of adding devices to an existing control system while it is running, and having the system (preferably automatically) utilize the new devices online, as “*Plug-and-Play Control*”.

While the idea of expanding a controller by adding to an existing control law is not, as such, new—see, e.g., [9], [10]—the subject of incorporating new *signals* or even subsystems into an existing system has not received much attention in the literature before. [11] and [12] used the “Plug and Play” terminology in a networked control framework, but the basic idea was quite different; it revolved around semi-autonomous agents and the emphasis was primarily on fault-tolerance. Furthermore, the overall concept presented in [11] and [12] seems to have more in common with the distributed optimization schemes of [13] than with the control design-oriented methodology proposed here, in the sense that the agents “communicate” through cost negotiations in an attempt to achieve global performance optimization.

Conceptually, Plug-and-Play control is somewhat related to “Windsurfer control” [14]–[16]. However, while Windsurfer control also aims for performance improvement by learning more about the plant during online operation, there have so far been no treatments of *structural* updates of the closed loop.

The main contribution of this paper is to *formulate the Plug-and-Play control problem* in a quite general setting. We also propose two possible approaches to the Plug-and-Play control problem, which can be deployed depending on the model information available and other criteria; however, we emphasize that these approaches are merely preliminary suggestions for solutions to the problem.

The general assumption is that the new control laws must be *added* to existing control laws when new sensors/actuators be-

Manuscript received December 23, 2010; revised June 14, 2011; accepted October 19, 2011. Manuscript received in final form October 25, 2011. Date of publication November 24, 2011; date of current version December 14, 2012. Recommended by Associate Editor J. Lu. This work was supported by The Danish Research Council for Technology and Production Sciences.

The authors are with the Department of Electronic Systems, Automation, and Control, Aalborg University, Aalborg 9220, Denmark (e-mail: ktr@es.aau.dk; dimon@es.aau.dk; jakob@es.aau.dk).

Color versions of one or more of the figures in this paper are available online at <http://ieeexplore.ieee.org>.

Digital Object Identifier 10.1109/TCST.2011.2174060

come available, while *leaving the existing control systems in place*. Also, we assume that an existing model is available, either from data-driven or from first-principles modeling.

When a device is added, the first step is to identify a model of it. As long as the new device does not involve significant dynamics, the added model can be identified in a fairly straightforward manner, see, e.g., [17]. If, on the other hand, the new device (sensor) involves dynamics, or if the measurement noise of the old and new sensors is correlated, the situation becomes more difficult. To this end, we briefly present a modified version of the so-called ‘‘Hansen scheme’’ for closed-loop system identification with open-loop-like qualities [18], [19]. With these techniques, it is possible to update the plant model without having to identify everything from scratch, and without having to decommission the plant in order to carry out dedicated experiments.

The paper then discusses two possible approaches to incorporating new devices into an existing control system in an ‘‘add-on’’ manner. The first approach is sensor fusion based, see, e.g., [20], [21]. There is a wide range of literature on implementation of controllers based on sensor fusion, see, e.g., [22] and the references therein. In the method presented here, however, we specifically address the situation of fusing new measurements with existing ones in order to modify the inputs to an existing controller, such that the overall performance is improved. To that end, an observer-based architecture is proposed, which can be carried out independently of the existing design.

The second method relies on the *Youla-Kucera* parametrization of all stabilizing controllers for a given plant. This methodology has the advantage that the performance transfer function is affine in the design parameter, which means that the design problem has an open-loop-like nature and good performance can thus be expected during the transition between controllers. Furthermore, certain stability guarantees can be given for this approach.

Both methods are tested in actual implementations; a climate control system for a livestock stable and a laboratory model of a district heating system. Note, however, that it is not our intention to provide a rigorous comparison between the methods, only to show that the Plug-and-Play control problem is feasible in practice.

After some preliminaries in Section II and a general problem statement in Section III, we discuss the identification issue in Section IV. Section V then outlines the Youla-Kucera-based control approach, while Section VI presents the sensor fusion-based control approach. Sections VII and VIII show the two practical application examples, and finally, Section IX sums up the conclusions of the work.

II. PRELIMINARIES

This section briefly recapitulates some basic concepts of coprime factorization and the Youla-Kucera parameterization of stabilizing controllers, which we will use extensively in the sequel; see [19], [23], [24], and [25] for further details. All results presented in this section are valid in either continuous and discrete time. Our notation is standard; $\mathcal{RH}_\infty^{p \times m}$ is the Banach

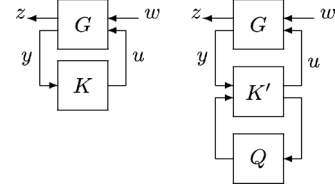


Fig. 1. (Left) The interconnection of the system G and the controller K . (Right) A different stabilizing controller implemented as $K(Q) = K' \star Q$, where K' is an augmented version of K , and Q is a *Youla-Kucera* parameter.

space of real rational stable transfer matrices mapping m -dimensional input signals to p -dimensional output signals, while \star denotes the so-called *star product* (feedback interconnection) between two LTI systems [26].

Consider the setup in the left block diagram in Fig. 1, where $w \in \mathbb{R}^{m_w}$ denotes external reference/noise input signals and $z \in \mathbb{R}^{p_z}$ represents performance outputs, e.g., deviations from reference values. $u \in \mathbb{R}^m$ and $y \in \mathbb{R}^p$ are controllable inputs and measurement outputs, respectively. G is the plant under consideration, while K is a controller. Let G be partitioned as

$$G = \begin{bmatrix} G_{zw} & G_{zu} \\ G_{yw} & G_{yu} \end{bmatrix}. \quad (1)$$

The closed loop is stable iff $G_{yu} \star K$ is stable. The LTI system G_{yu} can be factorized as

$$G_{yu} = NM^{-1} = \tilde{M}^{-1}\tilde{N} \quad (2)$$

with $N \in \mathcal{RH}_\infty^{p \times m}$, $M \in \mathcal{RH}_\infty^{m \times m}$, $\tilde{M} \in \mathcal{RH}_\infty^{p \times p}$, $\tilde{N} \in \mathcal{RH}_\infty^{p \times m}$. If the factors have no pole-zero cancellations, they are called *right* and *left coprime factorizations*, respectively. Correspondingly, K can be factorized as

$$K = UV^{-1} = \tilde{V}^{-1}\tilde{U} \quad (3)$$

where $U \in \mathcal{RH}_\infty^{m \times p}$, $V \in \mathcal{RH}_\infty^{p \times p}$, $\tilde{U} \in \mathcal{RH}_\infty^{m \times p}$, $\tilde{V} \in \mathcal{RH}_\infty^{m \times m}$. These coprime factorizations can be chosen to satisfy the double *Bezout identity*

$$\begin{bmatrix} \tilde{V} & -\tilde{U} \\ -\tilde{N} & \tilde{M} \end{bmatrix} \begin{bmatrix} M & U \\ N & V \end{bmatrix} = \begin{bmatrix} M & U \\ N & V \end{bmatrix} \begin{bmatrix} \tilde{V} & -\tilde{U} \\ -\tilde{N} & \tilde{M} \end{bmatrix} = \begin{bmatrix} I & 0 \\ 0 & I \end{bmatrix}. \quad (4)$$

The *Youla-Kucera parameterization* now states that *all* stabilizing controllers for some fixed system G_{yu} , and hence for G , based on some stabilizing K can be constructed by interconnecting K with a free, stable parameter system Q , as indicated in the right block diagram in Fig. 1.

In particular

$$K(Q) = (U + MQ)(V + NQ)^{-1} \\ = (\tilde{V} + Q\tilde{N})^{-1}(\tilde{U} + Q\tilde{M}), \quad Q \in \mathcal{RH}_\infty \quad (5)$$

where Q , which can be any stable system of appropriate input-output dimensions, is called the *Youla-Kucera parameter*. These configurations are illustrated in Fig. 2.

As pointed out in [27] and [28], by exploiting the Youla-Kucera parameterization, it is possible to change between two controllers online, say, from a nominal controller K_0 to another

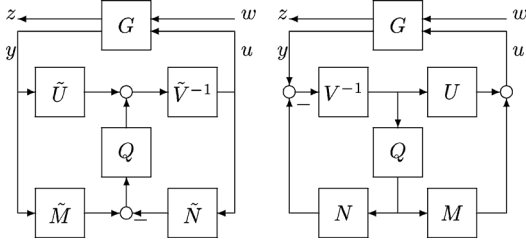


Fig. 2. Left and right coprime factorization-based Youla-Kucera parameterization of all stabilizing controllers.

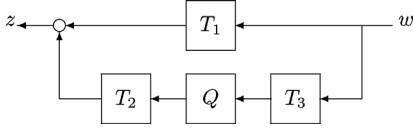


Fig. 3. Performance transfer function T_{zw} .

controller K_1 , in a smooth fashion by scaling the Q parameter by a scalar factor $\gamma \in [0; 1]$ without losing stability.

In fact, if a desired transfer function for a new stabilizing controller K_1 has been obtained, $K(Q) = K_1$ can be realized from K_0 and G by factoring $K_0 = \tilde{V}_0^{-1}\tilde{U}_0 = U_0V_0^{-1}$ and $K_1 = \tilde{V}_1^{-1}\tilde{U}_1 = U_1V_1^{-1}$ such that

$$\begin{bmatrix} \tilde{V}_1 & -\tilde{U}_1 \\ -\tilde{N} & \tilde{M} \end{bmatrix} \begin{bmatrix} M & U_1 \\ N & V_1 \end{bmatrix} = \begin{bmatrix} M & U_1 \\ N & V_1 \end{bmatrix} \begin{bmatrix} \tilde{V}_1 & -\tilde{U}_1 \\ -\tilde{N} & \tilde{M} \end{bmatrix} = \begin{bmatrix} I & 0 \\ 0 & I \end{bmatrix}$$

and setting (see [29])

$$Q = \tilde{U}_1V_0 - \tilde{V}_1U_0 = \tilde{V}_1(K_1 - K_0)V_0. \quad (6)$$

From Fig. 2 and using the Bezout identity, it is straightforward to see that

$$\begin{aligned} z &= G_{zw}w + G_{zu}(U + MQ)\tilde{M}G_{yw}w \\ &= G_{zw}w + G_{zu}M(U + Q\tilde{M})G_{yw}w \end{aligned}$$

i.e., the performance transfer function from w to z is affine in Q

$$T_{zw} = T_1 + T_2QT_3 \quad (7)$$

where T_1 , T_2 , and T_3 are stable transfer functions—see Fig. 3. Thus, given G and K , a control design can be carried out by finding a stable Q that minimizes T_{zw} in some sense. This is known as a model matching problem [30].

Once a Q has been designed, the affine dependence also means that if Q is scaled by γ as mentioned above, then the performance will change in a predictable way for all values of γ .

The Youla-Kucera parameterization has a *dual* formulation, which characterizes all (linear) plants stabilized by a (linear) controller. This formulation can be exploited to recast a closed-loop system identification problem (see Fig. 4) into an “open-loop-like” problem via the so-called “Hansen scheme” [18]. Doing so often leads to better-posed identification problems, since the input will then be uncorrelated with the noise.

Assume that a controller, factorized as $K = UV^{-1} = \tilde{V}^{-1}\tilde{U}$ stabilizes the plant we wish to identify, and that some nominal plant estimate G , factorized as $G = NM^{-1} = \tilde{M}^{-1}\tilde{N}$,

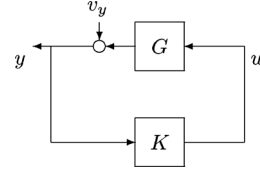


Fig. 4. Closed-loop system identification of a plant G in closed loop with a controller K . Due to the feedback, the input u is correlated with the noise v_y , making it difficult to identify G reliably.

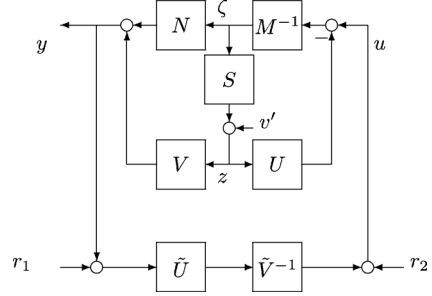


Fig. 5. Dual Youla-Kucera parameterization used for closed-loop system identification.

is known. Let the factorization be chosen to satisfy the Bezout identity (4). Then the dual Youla-Kucera parametrization of all plants stabilized by K can be represented as shown in Fig. 5, where S is a stable system denoted the dual Youla-Kucera parameter. In the figure, $v' = (\tilde{M} + S\tilde{U})v_y$ is the measurement noise that would normally affect the measurements y , relocated in the block diagram to affect the output of the dual Youla-Kucera parameter instead, and r_1 and r_2 are external excitation signals.

By manipulating the block diagram and using (4), it is possible to check that $y = G(S)u + v_y$. Furthermore, from the block diagram, we find the following relations:

$$(N + VS)\zeta = y - Vv' \quad (8)$$

and

$$(M + US)\zeta = u - Uv' = r_2 + \tilde{V}^{-1}\tilde{U}(y + r_1) - Uv'. \quad (9)$$

Applying the LTI operators \tilde{V} and \tilde{U} to (8) and (9), respectively, subtracting the bottom equation from the top equation and using the Bezout identity then results in

$$\zeta = \tilde{U}r_1 + \tilde{V}r_2. \quad (10)$$

In a similar vein, from the block diagram, we have the relations

$$M\zeta = u - Uz, \quad N\zeta = y - Vz.$$

Applying \tilde{N} to the top expression and \tilde{M} to the bottom one, subtracting one from the other and using the Bezout identity then results in

$$z = \tilde{M}y - \tilde{N}u \quad (11)$$

and, obviously, $z = S\zeta + v'$. ζ and z are thus available from filtered measurements. Furthermore, if v_y is independent of r_1 and r_2 , then ζ is independent of v' as well. Also, S is known to be

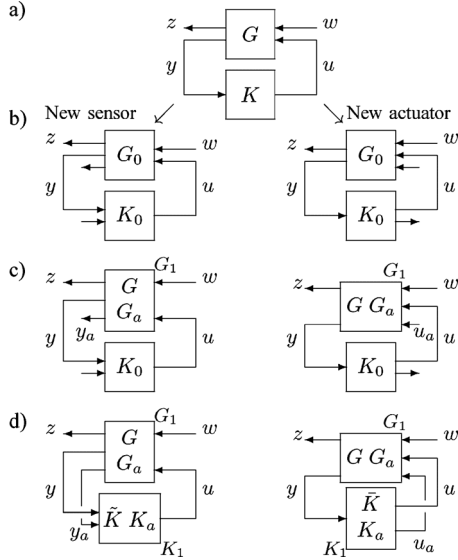


Fig. 6. Plugging in (left) a new sensor or (right) actuator. a) Initial situation. b) The existing system and controller are embedded in a non-minimal realization. c) (left) A new sensor or (right) actuator is added, providing access to a new measurement y_a or a new control signal u_a , respectively, yielding the extended plant G_1 . d) The controller is extended to include the new signal, yielding K_1 .

stable. Thus, it can be seen that although u and y are measured in closed-loop, the identification of S becomes equivalent to an open-loop identification problem. We shall utilize this technique in the sequel. See, e.g., [19] for more details, but please note that we are using positive feedback control here.

III. PROBLEM FORMULATION

We now turn our attention to the main problem treated in this paper. As mentioned in the introduction, the objective is to incorporate a new sensor or actuator in an existing control loop without having to re-design the existing system. There can be various reasons for this; for instance, the existing control system might contain supervisory logic that we do not wish to interfere with or replicate. Also, plant operators often tend to be wary of replacing a known, functioning controller with an entirely new replacement. Instead, adding a controller to the original one and slowly turning it on tends to be more appealing in practical applications.

Consider the situations depicted in Fig. 6.

The left column in Fig. 6 illustrates the situation where a new sensor is added, while the right column deals with adding an extra actuator. Let the existing system G have a minimal state space realization

$$G = \left[\begin{array}{c|cc} A & B_w & B \\ \hline C_z & D_{zw} & D_{zu} \\ C & D_{yw} & D \end{array} \right] \quad (12)$$

with $A \in \mathbb{R}^{n \times n}$, $B_w \in \mathbb{R}^{n \times m_w}$, $B \in \mathbb{R}^{n \times m}$, $C_z \in \mathbb{R}^{p_z \times n}$, $C \in \mathbb{R}^{p \times n}$, $D_{zw} \in \mathbb{R}^{p_z \times m_w}$, $D_{zu} \in \mathbb{R}^{p_z \times m}$, $D \in \mathbb{R}^{p \times m}$, and $D \in \mathbb{R}^{p \times m}$ being constant matrices, and let K be a stabilizing controller. For the sake of discussion, it will in the following

be assumed to be an observer-based state feedback controller of the form:

$$K = \left[\begin{array}{c|c} A + BF + LC + LDF & -L \\ \hline F & 0 \end{array} \right] \quad (13)$$

where the matrices F and L are chosen such that $A + BF$ and $A + LC$ have stable eigenvalues; however, it could in principle be any stabilizing LTI controller.

In both situations, the addition of the new device causes the *structure* of the closed loop to be changed. Since the input-output dimensions have to match, we embed the system and controller in a non-minimal realization before adding the new device (row b)). In the following, we only write out the case of adding a new sensor; adding a new actuator is dual, as also indicated by the use of similar symbols in both columns of Fig. 6.

The extended versions of G and K become

$$G_0 = \left[\begin{array}{c} G \\ 0 \end{array} \right] = \left[\begin{array}{cc|cc} A & 0 & B_w & B \\ A_{a1} & A_{a2} & 0 & B_a \\ \hline C_z & 0 & D_{zw} & D_{zu} \\ C & 0 & D_{yw} & D \\ 0 & 0 & 0 & 0 \end{array} \right] \quad (14)$$

and

$$K_0 = [K \quad 0] = \left[\begin{array}{c|cc} A + BF + LC + LDF & -L & 0 \\ \hline F & 0 & 0 \end{array} \right] \quad (15)$$

respectively. The new matrices are assumed to be real, constant matrices of appropriate dimensions chosen to accommodate the dimension of the added sensor signal and any dynamics that might be revealed when adding the new device (represented by A_{a1} and A_{a2}).

Note that $G \star K = G_0 \star K_0$, that is, we have not changed the closed-loop transfer function by this state space extension. Note also that G_0 is deliberately chosen such that the states corresponding to A_{a2} are unobservable.

Next, in row c), the new device is added, which causes G_0 to be replaced by the system

$$G_1 = \left[\begin{array}{c} G \\ G_a \end{array} \right] = \left[\begin{array}{cc|cc} A & 0 & B_w & B \\ A_{a1} & A_{a2} & 0 & B_a \\ \hline C_z & 0 & D_{zw} & D_{zu} \\ C & 0 & D_{yw} & D \\ C_{a1} & C_{a2} & D_{aw} & D_a \end{array} \right] \quad (16)$$

where C_{a1} , C_{a2} , D_{aw} , and D_a represent the output map of the new sensor. Note that these parameters are, in general, not known *a priori* and may thus require identification.

Finally, the problem we are faced with (in row d) of Fig. 6) is the following.

1) *Problem 1:* Design an extended controller $K_1 = [\bar{K} \quad K_a]$ (or $K_1 = \left[\begin{array}{c} \bar{K} \\ K_a \end{array} \right]$) that follows:

- utilizes the new measurement y_a (or control signal u_a);
- allows a *smooth transition* $K_0 \rightarrow K_1$, in the sense that the shift to the new controller should not cause large transients;

- retains closed-loop stability throughout the transition;
- allows recovering the old controller through the reverse transition $K_1 \rightarrow K_0$;

such that the performance transfer function T_{zw} is improved in some sense. \diamond

If the above problem is further restricted to be solved with minimal human intervention, we refer to it as *the Plug-and-Play Control Problem*.

IV. IDENTIFICATION OF NEW SENSOR

In order to solve Problem 1 in an automated way, it is often required to estimate the new parameters $A_{a1}, A_{a2}, \dots, D_a$ in the extended description above. Since we are not interested in stopping operation, the new parameter matrices must be identified online, while the plant is in closed-loop operation with the existing controller. Various approaches can be considered; in particular, if the new device is so fast that its dynamics is negligible compared to the general plant dynamics, the corresponding gains can be identified in a straightforward manner, see, e.g., [17]. If, on the other hand, the dynamics of the new sensor or actuator is not negligible, it will in many cases be advantageous to identify the new parameters in an open-loop-like setting. We briefly recount a possible approach, first suggested in [31].

A. Identifying a New Sensor

We focus on steps b) and c) in the left column of Fig. 6. The idea is to combine the Hansen Scheme (see Fig. 5) with the augmented plant and controller formulations introduced in the previous section, which means that we have to augment the coprime system and controller factors to accommodate the new measurement channels. It is reasonably straightforward to check that the following coprime factorizations correspond to (14)–(15), and satisfy the Bezout identity:

$$\begin{bmatrix} \tilde{M}_0 & U_0 \\ \tilde{N}_0 & V_0 \end{bmatrix} = \begin{bmatrix} A+BF & B & -L & 0 \\ F & I & 0 & 0 \\ \hline C+DF & D & I & 0 \\ 0 & 0 & 0 & I \end{bmatrix} \quad (17)$$

$$\begin{bmatrix} \tilde{V}_0 & -\tilde{U}_0 \\ -\tilde{N}_0 & \tilde{M}_0 \end{bmatrix} = \begin{bmatrix} A+LC & -(B+LD) & L & 0 \\ F & I & 0 & 0 \\ \hline C & -D & I & 0 \\ 0 & 0 & 0 & I \end{bmatrix} \quad (18)$$

for the system-controller pair before introducing the new sensor, and

$$\begin{bmatrix} M_1 & U_1 \\ N_1 & V_1 \end{bmatrix} = \begin{bmatrix} A+BF & 0 & B & -L & 0 \\ A_{a1}+B_aF & A_{a2} & B_a & 0 & 0 \\ \hline F & 0 & I & 0 & 0 \\ \hline C+DF & 0 & D & I & 0 \\ C_{a1}+D_aF & C_{a2} & D_a & 0 & I \end{bmatrix} \quad (19)$$

$$= \begin{bmatrix} \tilde{V}_1 & -\tilde{U}_1 \\ -\tilde{N}_1 & \tilde{M}_1 \end{bmatrix} = \begin{bmatrix} A+LC & 0 & -(B+LD) & L & 0 \\ A_{a1} & A_{a2} & -(B_a+LD_a) & 0 & 0 \\ \hline F & 0 & I & 0 & 0 \\ \hline C & 0 & -D & I & 0 \\ C_{a1} & C_{a2} & -D_a & 0 & I \end{bmatrix} \quad (20)$$

for the interconnection with the new sensor (dashed lines indicate which factors the respective matrices belong to).

The following result, which allows open-loop-like identification of the additional dynamics using a surprisingly simple dual Youla-Kucera parameter, was shown in [31].

Theorem 1: Consider the augmented plant (16) in closed loop with (15). The new sensor dynamics in the augmented plant G_1 is confined to a dual Youla-Kucera parameter S in Fig. 5 given by

$$S = \begin{bmatrix} A_{a2} & B_a & A_{a1} \\ C_{a2} & D_a & C_{a1} \end{bmatrix} \begin{bmatrix} A+BF & B \\ F & I \\ I & 0 \end{bmatrix}. \quad (21)$$

The identification procedure is straightforward; first generate a data sequence by adding excitation signals through r_1 and r_2 in Fig. 5, then compute the necessary signals ζ and z by filtering through the relevant factors, and compute the input to the unknown system by filtering ζ through the right (known) factor in (21). The left factor in (21) can now be obtained by a standard open-loop identification method.

B. Simulation Example

We illustrate the approach by a simple simulation example inspired by the application example considered in Section VIII, a simplified model of a livestock stable ventilation system. The example in the subsequent example, which concerns changing the control law after adding a sensor, is carried out on an actual

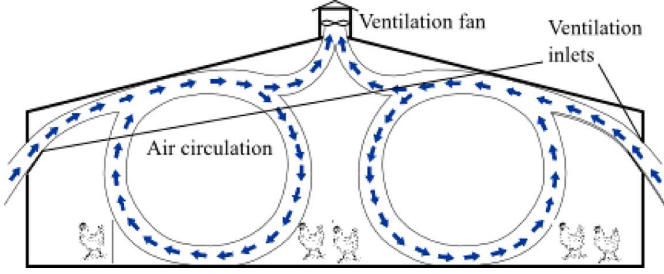


Fig. 7. Sketch of cross-section of the livestock stable. Fresh air enters the stable via inlets in the side, circulates within the stable and is eventually sucked out via the ventilation placed in the roof of the stable.

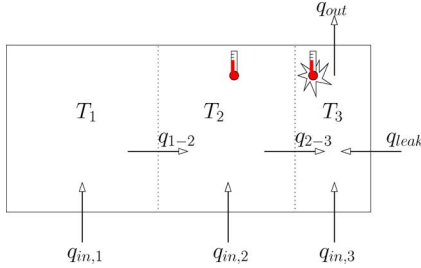


Fig. 8. Model setup used for the livestock stable simulation, with control volumes, air temperatures and airflows indicated. Initially, only T_2 is measured; later, the extra temperature sensor T_3 is installed to detect the temperature decrease caused by the leakage flow.

stable; in this example, however, we deliberately use a simulation model in order to have a “truth” model available for illustration purposes.

A vertical cross-section view of the stable is shown in Fig. 7. The figure gives a basic overview of how the ventilation part of the climate control system operates. Ventilation inlets in the walls of the stable are opened, allowing fresh air to enter. In the roof, a number of ventilation fans expel air to the surroundings. In combination, the inlets and outlets generate an air flow circulating within the stable, yield a comfortable temperature for the livestock in the stable and removes unhealthy gases such as ammonia. A single temperature sensor placed centrally within the stable is used for measurement feedback to a controller that controls the ventilation fan.

The simulation model is based on a simple zone division of the stable—see Fig. 8. Air flows in via inlets in the side walls, travels through the stable and exits via a chimney in zone 3. A temperature sensor in zone 2 is used for control of the flow q_{out} in the figure.

However, the livestock stable is not completely airtight. Due to cracks in the walls, etc., extra air tends to leak into the stable. This draft is not revealed by the temperature sensor T_2 because of its location; however, noticing that the livestock avoids one end of the stable, the farmer suspects that something is wrong and installs a new temperature sensor, T_3 , at the location indicated in Fig. 8. The task is now to identify the system parameters related to the new sensor while the system is operating.

Let $i = 1, 2, 3$ denote the zone number. m_i is the air mass in zone i , $q_{in,i}(t)$ is the inlet flow into zone i , $q_{out}(t)$ is the outlet flow, and $q_{i-j}(t)$ is the air flow from zone i to zone j at time t . In addition, there is a leak flow $q_{leak}(t)$ into zone 3.

Assuming the air is incompressible, we have the relation

$$q_{out}(t) = \sum_{i=1} q_{in,i}(t) + q_{leak}(t).$$

The inlets are fixed at given positions throughout the simulation. Hence, each inlet flow is given as a certain fixed percentage $0 < \alpha_i < 1$ of the outlet flow

$$q_{in,i}(t) = \alpha_i q_{out}(t), \quad q_{leak}(t) = \alpha_4 q_{out}(t).$$

Writing the mass and energy balances for each zone and linearizing the expressions around a suitable operating point, we obtain the system

$$\dot{x}(t) = \begin{bmatrix} -\frac{\bar{q}_{1-2}}{m_1} & 0 & 0 \\ \frac{\bar{q}_{1-2}}{m_2} & -\frac{\bar{q}_{2-3}}{m_2} & 0 \\ 0 & \frac{\bar{q}_{2-3}}{m_3} & -\frac{\bar{q}_{out}}{m_3} \end{bmatrix} x(t) + \begin{bmatrix} \alpha_1 \frac{\bar{T}_{amb} - \bar{T}_1}{m_1} \\ \alpha_2 \frac{\bar{T}_{amb} - \bar{T}_2}{m_2} \\ (\alpha_3 + \alpha_4) \frac{\bar{T}_{amb} - \bar{T}_3}{m_3} \end{bmatrix} u(t) + w(t) \quad (22)$$

$$y(t) = [0 \quad 1 \quad 0] x(t) + v(t). \quad (23)$$

Here, $(\bar{\cdot})$ denotes operating point values and $x(t) = [T_1(t) - \bar{T}_1, T_2(t) - \bar{T}_2, T_3(t) - \bar{T}_3]^T$, $y(t) = T_2(t) - \bar{T}_2$ and $u(t) = q_{out}(t) - \bar{q}_{out}$ denote deviations from the operating points (“small-signals”). The animals are assumed to deliver a stochastic heat input with a constant bias, which can be treated as an extra addition to the zone temperature operating point $[\bar{T}_1, \bar{T}_2, \bar{T}_3]^T$; hence, $w(t)$ and $v(t)$ can be considered zero-mean noise sequences.

Appropriate parameter and operating point values are substituted into the model, which is sampled using zero-order hold with a sampling period of 10 s. However, since the leakage flow was not taken into consideration at the design time, and the original temperature sensor is placed in zone 2 (centrally in the stable), the controller is designed based on the (x_1, x_2) -subsystem

$$\begin{bmatrix} x_1(t+1) \\ x_2(t+1) \end{bmatrix} = \begin{bmatrix} 0.9265 & 0 \\ 0.0693 & 0.8892 \end{bmatrix} \begin{bmatrix} x_1(t) \\ x_2(t) \end{bmatrix} + \begin{bmatrix} -0.1737 \\ -0.009814 \end{bmatrix} u(t) + \begin{bmatrix} w_1(t) \\ v_2(t) \end{bmatrix} \quad (24)$$

$$y(t) = [0 \quad 1] x(t) + v_y(t). \quad (25)$$

This system represents the known model, with known noise statistics

$$R_w = \begin{bmatrix} 0.02 & 0.01 \\ 0.01 & 0.02 \end{bmatrix} \quad R_{v_y} = 0.1.$$

An observer-based state feedback controller with $F = [0.4628 \ 1.8625]$ and $L = [-0.2307 \ -0.3306]^T$ is applied to maintain the temperature in zone 2 at a setpoint of 21 °C.

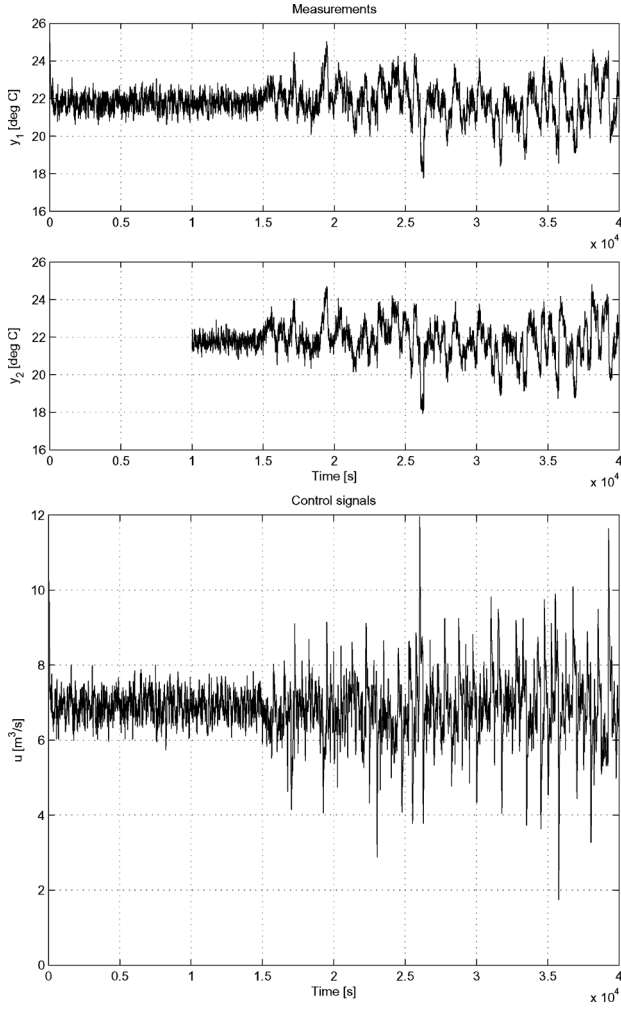


Fig. 9. Closed-loop simulation. The extra temperature sensor T_3 is activated after 2000 samples. (Top) temperature measurements; (bottom) control signal.

When the new temperature sensor is added, it becomes possible to observe the last state in the true simulation model

$$x(t+1) = \begin{bmatrix} 0.9265 & 0 & 0 \\ 0.0693 & 0.8892 & 0 \\ 0.01087 & 0.2657 & 0.6333 \end{bmatrix} x(t) + \begin{bmatrix} -0.1737 \\ -0.009814 \\ -0.213 \end{bmatrix} u(t) + w(t) \quad (26)$$

$$y(t) = [0 \ 1 \ 0] x(t) + v_y(t) \quad (27)$$

$$y_a(t) = [0 \ 0 \ 1] x(t) + v_a(t) \quad (28)$$

with noise statistics

$$R_w = \begin{bmatrix} 0.02 & 0.01 & 0 \\ 0.01 & 0.02 & 0.01 \\ 0 & 0.01 & 0.03 \end{bmatrix} \quad R_{v_y v_a} = \begin{bmatrix} 0.1 & 0.05 \\ 0.05 & 0.07 \end{bmatrix}. \quad (29)$$

The state and measurement noise are uncorrelated.

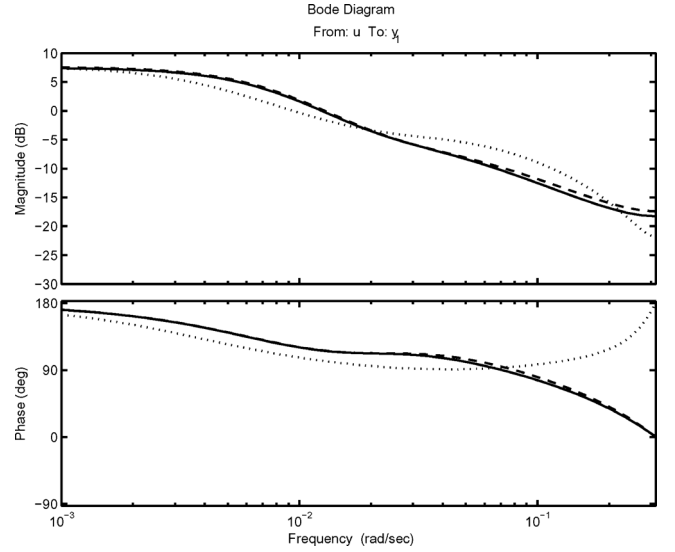


Fig. 10. Bode plots of the identified models. (Solid line) Real. (Dashed line) Hansen. (Dotted line) Direct identification. Note how the Hansen scheme provides much improved identification at higher frequencies compared to direct identification.

Excitation is added to the reference and the input in the form of steps with a length of 250 s. Various levels and periods of excitation are examined. One example is shown in Fig. 9.

At 10 000 s, the new sensor is introduced, and from 15 000 s onwards, one hundred steps of random amplitude with standard deviation 1 are applied as excitation on the reference and the input. This level of excitation causes deviations in temperature that would be acceptable for a short time. Models of the new sensor is now obtained by the following:

- performing a direct system identification on input and output measurements, as if they had been generated in open loop;
- using the Hansen scheme presented above to extend the model dynamics.

The actual system identification was carried out using MATLAB's N4SID toolbox, but any standard system identification procedure could in principle be applied.

Fig. 10 compares the results to the actual simulation model. The direct method tends to give a result that would be unreliable for controller design, as in this example. The frequency response of the model produced by the Hansen scheme gets very close to that of the real system, on the other hand.

In order to make a more thorough evaluation of the robustness of the schemes, a number of tests with varying levels and lengths of excitation are made. The quality of the models are evaluated by the unweighted ν -gap between the identified model and the real simulation model. The ν -gap expresses the difference between two transfer functions in terms of their similarity with respect to closed loop operation; that is, if the ν -gap between two plant models is small, then a good controller designed for one transfer function will also work well with the other [32].

Fig. 11 shows the results for three different levels of excitation. In the left-most plot, the steps have standard deviation of 0.1, which means that they are hardly distinguishable from the

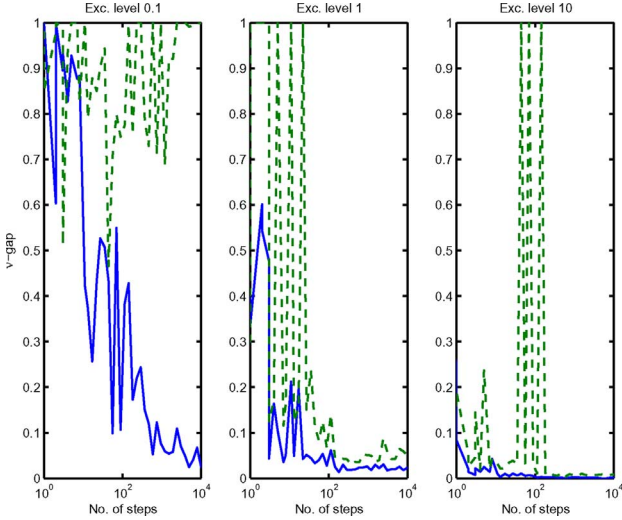


Fig. 11. ν -gap between identified models and real system obtained at three different levels of excitation; from left to right, the standard deviation of the excitation signals is 0.1, 1, and 10, respectively. The x -axis indicates the number of steps in the excitation sequence. (Solid line) Hansen. (Dotted line) Direct identification.

noise level. The x -axis indicates the number of steps in the excitation sequence. For the Hansen scheme, a few hundred steps are enough to ensure a reliable model. The direct identification method gives basically useless results for any number of steps.

In the middle plot, the excitation has standard deviation 1, just as in the simulation shown above. Now the Hansen scheme gives reliable results even for a very short excitation sequence, whereas thousands of steps are needed in order for the direct method to yield trustworthy results.

In the right-most plot, the steps have standard deviation of 10, which would be entirely unrealistic in a real livestock stable. Now only a couple of steps are necessary for the Hansen scheme, but the direct identification method can go wrong even with 30 steps, thus illustrating that closed-loop identification is quite troublesome for systems like the one considered here.

V. YOULA-KUCERA-BASED CONTROLLER MODIFICATION

Assuming that a model for the added device is in place, we will from now on turn our attention to designing an additive controller that exploits the new information in a meaningful manner.

Note that Problem 1 does not impose any restrictions on how the extension shall be added to the existing control. Indeed, if full access to the internal structure of the existing controller is available, (6) provides a straightforward expression for computing the transfer function needed to shift from the old to the new controller. Although not directly treating Plug-and-Play control, [29] provides convenient state space formulae for realizing a new controller based on an existing one, which may be employed with little to no modification.

However, there are many cases where we wish to introduce the new controller by accessing only the *terminals* of the existing controller. This may for instance occur because the existing controller is implemented in a dedicated microprocessor

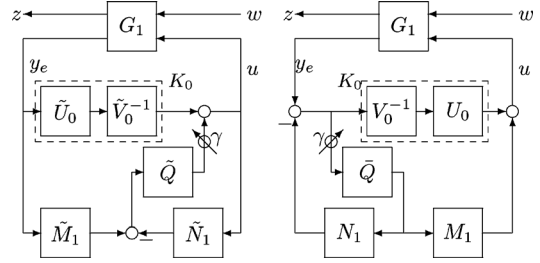


Fig. 12. Controller parameterization modified for connection to terminals of existing controller; note that $\tilde{Q} \neq \bar{Q}$.

that does not permit modifications of source code, or the internal states of the controller are not available for other reasons. Accessing only the terminals has the added advantage that it is very easy to remove the control extension again, should the need arise.

In this and the following sections, we suggest two different approaches to Problem 1 that only access the terminals of the existing controller. Motivated by its inherent stability features, the first method of controller reconfiguration utilizes the Youla-Kucera factorization.

Inspecting Fig. 2, it is seen that there are two possible ways to modify the Youla-Kucera parameterization in the desired manner. They are shown in Fig. 12.

Recall that, in the case of a new sensor, $K_0 = [K \ 0]$; thus, the original controller is kept in place and is only accessed at the terminals. Stability of \tilde{Q} resp. \bar{Q} still implies stability of the closed loop, but now it is no longer *all* stabilizing controllers that can be found by inserting stable \tilde{Q} resp. \bar{Q} .

In [33], the following theorem was presented.

Theorem 2: Let $\tilde{M}_1^{-1}\tilde{N}_1$ be a coprime factorization of the LTI system G_1 , and assume that $K_0 = \tilde{V}_0^{-1}\tilde{U}_0 = U_0V_0^{-1}$ is a stabilizing controller, i.e., $G_1 \star K_0 \in \mathcal{RH}_\infty$. Assume a second controller $K_1 = \tilde{V}_1^{-1}\tilde{U}_1 = U_1V_1^{-1}$ is given. Then

$$G_1 \star K_1 \in \mathcal{RH}_\infty \wedge V_0^{-1}V_1 \in \mathcal{RH}_\infty \quad (30)$$

is equivalent to the existence of a stable \tilde{Q} such that

$$K_1 = (I + \tilde{Q}\tilde{N}_1)^{-1}(K_0 + \tilde{Q}\tilde{M}_1) \quad (31)$$

i.e., (31) is a parameterization of all stabilizing controllers that include the right half plane pole structure of K_0 .

Proof: See [33]. ■

The parameterization above corresponds to the left part of Fig. 12. In some cases, the right part is more useful, however, and we therefore present the corresponding theorem:

Theorem 3: Let $N_1M_1^{-1}$ be a coprime factorization of the LTI system G_1 , and assume that $K_0 = \tilde{V}_0^{-1}\tilde{U}_0 = U_0V_0^{-1}$ is a stabilizing controller, i.e., $G_1 \star K_0 \in \mathcal{RH}_\infty$. Assume a second controller $K_1 = \tilde{V}_1^{-1}\tilde{U}_1 = U_1V_1^{-1}$ is given. Then

$$G_1 \star K_1 \in \mathcal{RH}_\infty \wedge \tilde{V}_1\tilde{V}_0^{-1} \in \mathcal{RH}_\infty \quad (32)$$

is equivalent to the existence of a stable \bar{Q} such that

$$K_1 = (K_0 + M_1\bar{Q})(I + N_1\bar{Q})^{-1} \quad (33)$$

i.e., (33) is a parameterization of all stabilizing controllers that include the right half plane pole structure of K_0 .

Proof: First, assume that a controller K_1 satisfying (32) is given where, without loss of generality, we can assume that the parameterizations given satisfy the double Bezout identity. Define

$$\bar{Q} = \tilde{U}_1 - \tilde{V}_1 \tilde{V}_0^{-1} \tilde{U}_0.$$

Equation (32) implies that \bar{Q} is stable. Inserting \bar{Q} in (33) yields

$$\begin{aligned} & (K_0 + M_1 \bar{Q})(I + N_1 \bar{Q})^{-1} \\ &= (K_0 + M_1(\tilde{U}_1 - \tilde{V}_1 \tilde{V}_0^{-1} \tilde{U}_0)) \times (I + N_1(\tilde{U}_1 - \tilde{V}_1 \tilde{V}_0^{-1} \tilde{U}_0))^{-1} \\ &= (\tilde{V}_0^{-1} \tilde{U}_0 + M_1 \tilde{U}_1 - M_1 \tilde{V}_1 \tilde{V}_0^{-1} \tilde{U}_0) \\ & \quad \times (\tilde{V}_1 \tilde{M}_1 - N_1 \tilde{V}_1 \tilde{V}_0^{-1} \tilde{U}_0)^{-1} \\ &= (U_1 \tilde{M}_1 - U_1 \tilde{N}_1 \tilde{V}_0^{-1} \tilde{U}_0)(V_1 \tilde{M}_1 - V_1 \tilde{N}_1 \tilde{V}_0^{-1} \tilde{U}_0)^{-1} \\ &= U_1(\tilde{M}_1 - \tilde{N}_1 \tilde{V}_0^{-1} \tilde{U}_0)(\tilde{M}_1 - \tilde{N}_1 \tilde{V}_0^{-1} \tilde{U}_0)^{-1} V_1^{-1} \\ &= U_1 V_1^{-1} = K_1. \end{aligned}$$

Conversely, assume that K_1 is given by

$$K_1 = (K_0 + M_1 \bar{Q})(I + N_1 \bar{Q})^{-1}. \quad (34)$$

We rewrite (34) as

$$\begin{aligned} K_1 &= (U_0 V_0^{-1} + M_1 \bar{Q})(I + N_1 \bar{Q})^{-1} \\ &= (U_0 + M_1 \bar{Q} V_0)(V_0 + N_1 \bar{Q} V_0)^{-1} \\ &= (U_0 + M_1 Q)(V_0 + N_1 Q)^{-1} \end{aligned}$$

with $Q = \bar{Q} V_0 \in \mathcal{RH}_\infty$, and we see that K_1 is a stabilizing controller by comparing with (5).

In order to prove that \tilde{V}_1 contains the RHP zero structure of \tilde{V}_0 , we rearrange (34) into

$$\tilde{V}_1^{-1} \tilde{U}_1 (I + N_1 \bar{Q}) = (\tilde{V}_0^{-1} \tilde{U}_0 + M_1 \bar{Q})$$

and further into

$$\tilde{U}_1 (I + N_1 \bar{Q}) - \tilde{V}_1 M_1 \bar{Q} = \tilde{V}_1 \tilde{V}_0^{-1} \tilde{U}_0. \quad (35)$$

Since the left-hand side of (35) is stable, so is the right hand side. Due to coprimeness of \tilde{U}_0 and \tilde{V}_0 no RHP cancellations occur when forming the product $\tilde{V}_0^{-1} \tilde{U}_0$, and since \tilde{V}_1 is stable, the product $\tilde{V}_1 \tilde{V}_0^{-1}$ itself must be stable. ■

To sum up, we can modify the controller at the terminals to obtain some new desired controller K_1 , provided that we can find coprime factors for K_1 fulfilling the Bezout identity and either (32) or (30). If these assumptions are satisfied, we can either find a stable \bar{Q} solving

$$\bar{Q} V_0 = \tilde{U}_1 V_0 - \tilde{V}_1 U_0 = \tilde{V}_1 (K_1 - K_0) V_0 \quad (36)$$

or a stable \tilde{Q} solving

$$\tilde{V}_0 \tilde{Q} = \tilde{U}_1 V_0 - \tilde{V}_1 U_0 = \tilde{V}_1 (K_1 - K_0) V_0 \quad (37)$$

respectively. Then we can construct the appropriate controller shown in the block diagrams in Fig. 12, and by gradually increasing γ from 0 to 1, the overall behavior from y to u changes smoothly from K_0 to K_1 without losing stability for any value of γ .

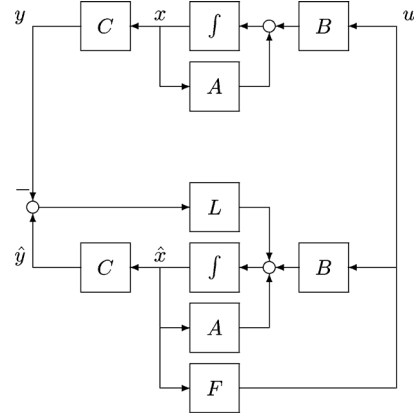


Fig. 13. Existing system G and controller K .

Remark 2: The interpretation of the second condition of (32) is that the two controllers have to have the same (closed) right-half plane poles in open loop, as the structure would otherwise cause a RHP pole-zero cancellation. ◁

Remark 3: Note that for a given desired controller K_1 , it is not given that both (32) or (30) can be fulfilled. In some cases, it will only be possible to satisfy one of them. In such case we can then only pick the corresponding terminal connection in Fig. 12. In general, if the number of (plant) outputs is higher than the number of inputs, then (32) is easier to fulfill, and correspondingly (30) is easier to fulfill for a higher number of inputs. ◁

Remark 4: If for some given desired K_1 we cannot find a stable \bar{Q} or \tilde{Q} fulfilling (32) or (30), respectively, one might instead consider finding approximate stable solutions to (36) or (37). ◁

VI. SENSOR FUSION-BASED APPROACH

In this approach, we replace the inputs to the existing controller with new inputs, which are computed from both the existing and additional measurements. Consider the system shown in Fig. 13, which is exactly an implementation of the plant-controller interconnection (12)–(13) before augmentation (albeit ignoring the performance channels).

Now we assume that a new sensor becomes available, which can provide measurements of higher quality of one or more of the plant states, e.g., with less measurement noise. Rather than re-designing and re-commissioning the entire system, we introduce the extra measurements through a pre-filter in the hope that the better measurement quality will manifest itself in better closed-loop performance, for instance in terms of better disturbance rejection. Note that it is assumed that the sensor has no significant dynamics, and that a model for it is known.

The augmented system is described by a state-space model of the form

$$G_1 = \left[\begin{array}{c|c} A & B \\ \hline C & 0 \\ C_a & 0 \end{array} \right] = \left[\begin{array}{c|c} A & B \\ \hline C_e & 0 \end{array} \right] \quad (38)$$

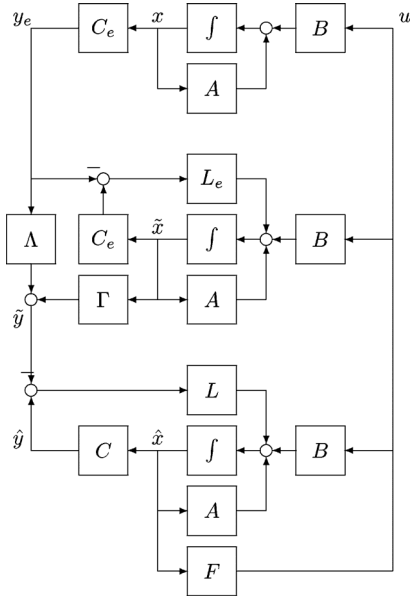


Fig. 14. Architecture for $G_1 \star K_1$ with additional observer.

where

$$C_e = \begin{bmatrix} C \\ C_a \end{bmatrix} \in \mathbb{R}^{(p+p_a) \times n}.$$

Furthermore, let

$$y_e = \begin{bmatrix} y \\ y_a \end{bmatrix} \in \mathbb{R}^{p+p_a}$$

denote the extended measurement vector. In order to exploit the new outputs, an additional observer is introduced as shown in Fig. 14

$$\dot{\tilde{x}} = A\tilde{x} + Bu + L_e(C_e\tilde{x} - y_e) \quad (39)$$

$$\tilde{y} = \Gamma\tilde{x} + \Lambda y_e \quad (40)$$

where $L_e \in \mathbb{R}^{n \times (p+p_a)}$, $\Gamma \in \mathbb{R}^{p \times n}$ and $\Lambda \in \mathbb{R}^{p \times (p+p_a)}$ are design parameters (see below). L_e must be chosen such that $A + L_e C_e$ is Hurwitz; furthermore, it is clear that by choosing

$$\Lambda = [I \ 0], \quad \Gamma = 0$$

we have $\tilde{y} = y$ and the original closed loop is recovered.

We have the following separation principle for the proposed architecture.

Theorem 4: Consider the configuration illustrated by Fig. 14, where a system given by the state space model (38) is controlled by an observer based compensator, designed for an original system (12), and the input to the controller is generated by an additional observer of the form (39).

This closed-loop system has poles given by the eigenvalues of the two matrices

$$A + L_e C_e, \quad \begin{bmatrix} A + BF & BF \\ L(C - \Gamma - \Lambda C_e) & A + LC \end{bmatrix}.$$

In the special case where Γ and Λ are chosen to fulfill

$$\Gamma + \Lambda C_e = C \quad (41)$$

the closed-loop system satisfies a “full” separation principle, i.e., the closed-loop poles are given by the eigenvalues of the three matrices

$$A + BF, \quad A + L_e C_e, \quad A + LC$$

which means that the observer and feedback gains can be designed independently, if only the closed-loop poles are of concern.

Proof: See [34]. ■

The intuition for the condition (41) is that the new input to the original controller is generated as an interpolation between the original measurements and an estimate of the original measurements based on the original and the new measurements. Therefore, if the new measurements are of a poor quality, i.e., the signal-to-noise ratio is low, we may place stronger emphasis on the old measurements by choosing

$$\Lambda C_e \approx C, \quad \Gamma \approx 0$$

while still satisfying (41). On the other hand, if the new measurements are highly superior to the original measurements, we may choose

$$\Lambda \approx 0, \quad \Gamma \approx C.$$

Remark 5: Although Theorem 4 suggests that the new observer can be designed independently of the existing controller, it should be noted that the new observer can introduce a significant phase shift, which should be taken into consideration in the design process. In fact, as will be demonstrated in Section VII, it may sometimes be advantageous to choose Γ and Λ such that (41) is not satisfied. ◁

Remark 6: It should also be noted, that if (41) is not satisfied, \tilde{x} is still an estimate of x , whereas \hat{x} cannot be assumed to be an estimate of x . Thus, if the original controller depends on a reliable state estimate, then Γ and Λ should indeed be chosen to satisfy (41). ◁

Remark 7: It is not in itself surprising that a better result can be achieved if (41) is not imposed as a constraint. In that case, the combined new controller, consisting of the original controller and the new observer, is allowed to increase the overall gains of the system, based on the improved measurement situation. The main disadvantage of pursuing a design that does not satisfy (41) is that the link between design parameters and design objectives becomes more complicated, and some sort of optimization procedure will typically be required for the design, which may be non-trivial. To sum up, the optimal choice of Γ and Λ is an open problem. ◁

VII. DISTRICT HEATING SYSTEM CONTROL

In the following, the methods presented in the two preceding sections will be demonstrated on actual plants, first a laboratory experiment on a district heating system model and then a live-stock stable. Note that the methods are not compared directly, since the experiments mainly serve as proof-of-concept.



Fig. 15. Test setup.

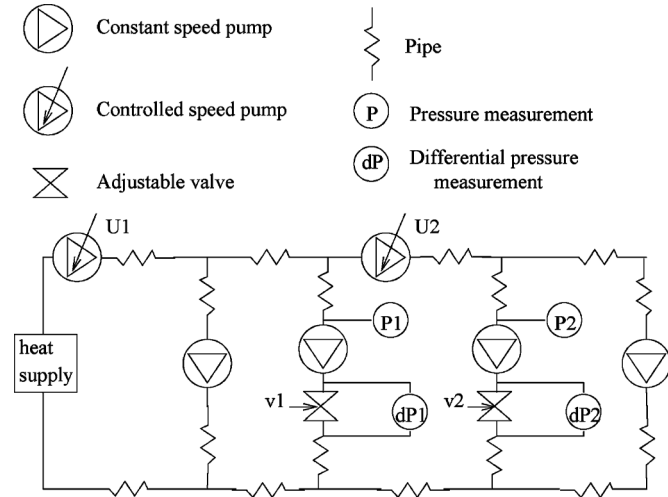


Fig. 16. Structure of the test setup.

A. System Description

The test setup shown in Fig. 15 is a scaled-down model of a district heating system. The dynamical behavior is similar to a real system, except that the time constants are approximately ten times faster. For further details on pipe lengths, etc., see [35].

The configuration used in this example is shown in Fig. 16. Note that all the signals in the figure are scalars, sampled with a sampling time of 0.5 s.

The heat entering at the supply is distributed to the four consumer branches using six pumps. The two middle consumers have varying consumption, which is modeled by adjustable valves, v_1 and v_2 . In this example, the task of the control system is to maintain constant differential pressures, $dP_1 = dP_2 = 0.1$ bar.

The test setup provides measurements of the two valve positions, two differential pressures and two pressures (relative to ambient atmospheric pressure).

The valve movements follow a simulated heat consumption, but are affected by a slew rate and hysteresis, resulting in the behavior seen in the top row of Fig. 17 (solid lines). These valve positions are not available to the controller, but can to some extent be estimated from measurements.

The controllers are based on a model obtained through system identification from open-loop data. The model consists of a third

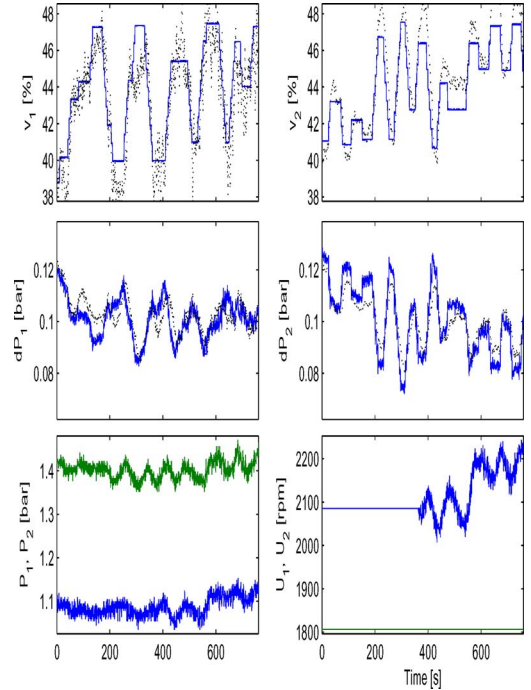


Fig. 17. Performance of initial controller, switched on at 360 s. Full lines indicate measurements, while dotted lines indicate estimates. (Top row) Valve settings; (middle row) differential pressures; (bottom row) outputs and control signals.

order innovations model of the transfer function from pump speeds and valve settings to pressures and differential pressures. The valves are modeled as white noise filtered through first-order filters, resulting in a model of the form

$$\begin{aligned}
 x(t+1) &= Ax(t) + B \begin{bmatrix} U_1^\delta(t) \\ U_2^\delta(t) \end{bmatrix} + \begin{bmatrix} K_P e_P(t) + K_{dP} e_{dP}(t) \\ K_v e_v(t) \end{bmatrix} \\
 y_P(t) &= C_P x(t) + e_P(t) \\
 y_{dP}(t) &= C_{dP} x(t) + e_{dP}(t)
 \end{aligned}$$

where $x(t) = [x_1(t) \ x_2(t) \ x_3(t) \ v_1^\delta(t) \ v_2^\delta(t)]^T$ are state and valve setting estimates and $e_P(t)$, $e_{dP}(t)$ and $e_v(t)$ are innovations (one-step prediction errors) for $P(t) = [P_1(t) \ P_2(t)]^T$, $dP(t) = [dP_1(t) \ dP_2(t)]^T$, and $v(t) = [v_1^\delta(t) \ v_2^\delta(t)]^T$, respectively. $(\cdot)^\delta$ denotes “small-signals,” i.e., deviations from operating points. The model parameters are as follows:

$$\begin{aligned}
 A &= \begin{bmatrix} 0.721 & -0.00251 & 0.0489 & -0.029 & -0.0497 \\ -0.00669 & 0.69 & -0.00249 & 0.0316 & -0.0327 \\ 0.0921 & 0.0172 & 0.923 & -0.0342 & -0.0826 \\ 0 & 0 & 0 & 0.997 & 0 \\ 0 & 0 & 0 & 0 & 0.997 \end{bmatrix} \\
 B &= \begin{bmatrix} 0.161 & 0.0544 \\ -0.0592 & 0.17 \\ -0.0593 & -0.0267 \\ 0 & 0 \\ 0 & 0 \end{bmatrix} \\
 K_P &= \begin{bmatrix} -0.0123 & -0.00597 \\ -0.0252 & 0.0202 \\ -0.132 & -0.136 \end{bmatrix}
 \end{aligned}$$

$$K_{dP} = \begin{bmatrix} 0.338 & 0.409 \\ -0.362 & 0.268 \\ 1.24 & 1.38 \end{bmatrix}$$

$$C_P = \begin{bmatrix} 1.97 & -1.06 & -0.427 & 0 & 0 \\ 2.51 & 1.16 & -0.471 & 0 & 0 \end{bmatrix}$$

$$C_{dP} = \begin{bmatrix} 0.478 & -0.473 & 0.0615 & 0 & 0 \\ 0.514 & 0.319 & 0.0766 & 0 & 0 \end{bmatrix}.$$

Furthermore, the estimated noise covariances are

$$E \left\{ \begin{bmatrix} e_P \\ e_{dP} \end{bmatrix} \begin{bmatrix} e_P \\ e_{dP} \end{bmatrix}^T \right\}$$

$$= 10^{-4} \times \begin{bmatrix} 0.192 & -0.0915 & 0.126 & 0.235 \\ -0.0915 & 0.19 & 0.189 & 0.0426 \\ 0.126 & 0.189 & 2.71 & 0.834 \\ 0.235 & 0.0426 & 0.834 & 2.47 \end{bmatrix}$$

$$E\{e_v e_v^T\} = 10^{-6} \times \begin{bmatrix} 2.8 & 0 \\ 0 & 2.57 \end{bmatrix}.$$

As system identification is not central to this example, we will omit further details; the model will only be used for controller design.

B. Initial Controller

Initially, the differential pressure measurements are not available to the control system, which relies on $y_P(t) = [P_1(t) \ P_2(t)]^T$ only. Also, the pump U_2 is a constant-speed pump, so the controlled system has two outputs and a single input. The controller is designed as an LQG controller penalizing the (estimated) differential pressures, i.e., $Q_{SF} = C_{dP}^T C_{dP}$, and the control signal $R_{SF} = 10^{-4}$.

Fig. 17 compares open-loop and initial closed-loop operation. The first four plots show the valve positions and the differential pressures. These are not available to the controller, but the observer can to some extent reconstruct them, as shown by the dotted lines. The next plots show the measured pressures and the resulting control signals, i.e., pump speeds.

C. Adding Sensors

Even though the estimates are not very accurate, the controller is able to decrease the variation of the differential pressures. However, the consumers complain about varying supply rates, so the differential pressure sensors are added to examine the problem and see if the control can be improved. Thus, the measurement vector is now expanded to

$$y_e(t) = \begin{bmatrix} y_P(t) \\ y_{dP}(t) \end{bmatrix}.$$

We first employ the sensor fusion method described in Section VI. We design the new observer gain L_e as LQ-optimal according to the model. It quickly becomes clear that almost no change in controller behavior can be achieved by fulfilling the “full” separation constraint (41). Instead, we set $\Lambda = [I \ 0]$ and $\Gamma = [0 \ \gamma_v]$, where $\gamma_v \in \mathbb{R}^{2 \times 2}$ acts as a feedforward

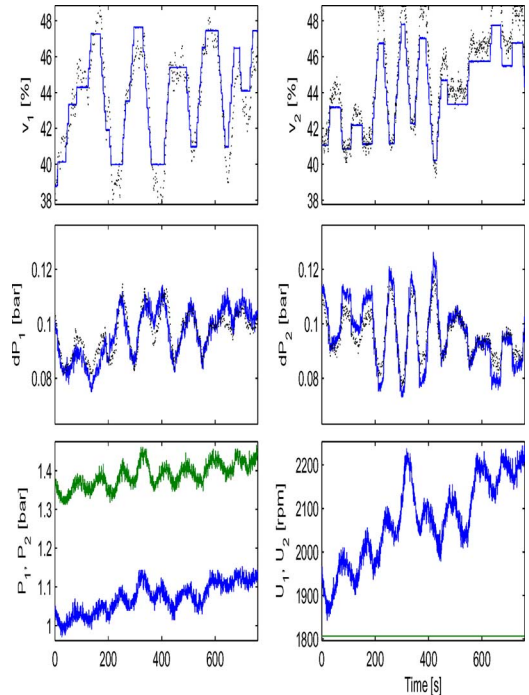


Fig. 18. Performance of controller with additional observer. Full lines indicate measurements, while dotted lines indicate estimates. (Top row) valve settings; (middle row) differential pressures; (bottom row) outputs and control signals.

gain from the valve position estimates and is found from simulations to yield the same steady-state errors as would have been achieved by replacing the internal observer in the original controller.

From the simulations it is also clear that only small improvements will be achieved, and this is indeed also seen in the resulting plot in Fig. 18. Comparing with the last half of Fig. 17, the changes are difficult to identify (note that the valve sequence is approximately the same). On the other hand, the new measurements improve not just the estimates of the differential pressures, but also the estimates of the valve position (the dotted lines show the estimates in the additional observer).

D. Adding an Actuator

Since the additional sensors revealed a problem with the performance, it is decided to add control capabilities to the U_2 pump, enabling us to control the speed. The sensor fusion filter is removed, and instead the modification method in Section V is applied, choosing the right-side configuration in Fig. 12.

An optimal controller K_1 is designed for the system with four measurements and two control inputs. Since the original controller K_0 has an unstable pole in 1.06, K_1 cannot be realized exactly. Instead, the unstable \bar{Q} found from (36) is approximated by separating the unstable part and flipping the unstable pole inside the unit circle. This results in a somewhat different controller from the optimal, but the theory guarantees stability as long the model is correct, so it is decided to test it.

The result is shown in Fig. 19. Between 300 and 400 s the scheduling parameter γ is increased from 0 to 1, modifying the

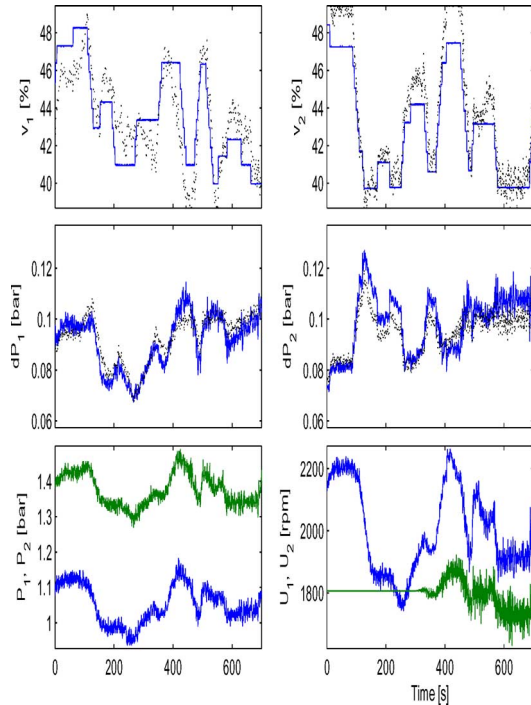


Fig. 19. Performance of controller with terminal addition. Full lines indicate measurements, while dotted lines indicate estimates. Top row: valve settings; middle row: differential pressures; bottom row: outputs and control signals. From time 300 to 400 s, the controller is gradually transformed the existing to a new controller that exploits the new measurements. Stability is maintained throughout the transition, and performance is improved, in particular for dP_2 (the deviation from the reference value of 0.1 bar is significantly reduced compared to $t < 300$ s).

controller to use the new sensors and the new actuator. This results in a much better performance, especially for dP_2 .

VIII. LIVESTOCK STABLE CONTROL

Finally, we document a real-life experiment where the Youla-Kucera-based approach introduced in Section V was employed to utilize a new temperature sensor measurement. The test was carried out on a livestock stable located in Northern Jutland, Denmark (see Fig. 20). See [36] for further details on the test stable and the specific controller implementation.

Fig. 21 shows the nominal operation of the existing control system. A single temperature sensor, T_0 , is used for measurement feedback to a PI controller that controls the ventilation fans indicated on the figure. The controller maintains a fixed temperature. The situation is thus quite similar to the simulation example in Section IV, except that a zone model is not used in the current case.

The livestock stable is not completely airtight. Due to cracks in the walls, etc., extra air tends to leak into the stable; in Fig. 22, this extra draft is indicated by faded arrows at the left end of the stable. This draft cannot be detected by T_0 , but the farmer observes that the livestock avoids that area and installs a new temperature sensor, T_1 , at the location indicated in the figure.

In the given system, the ventilation rate serves as a single input. We would thus like to reconfigure from a SISO controller to a one-by-two controller. Ideally, we would like zero steady

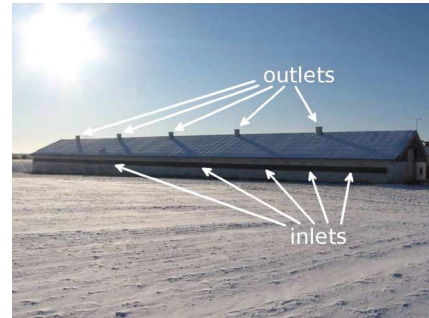


Fig. 20. Photograph of the livestock stable used for the experiments in Section VIII.

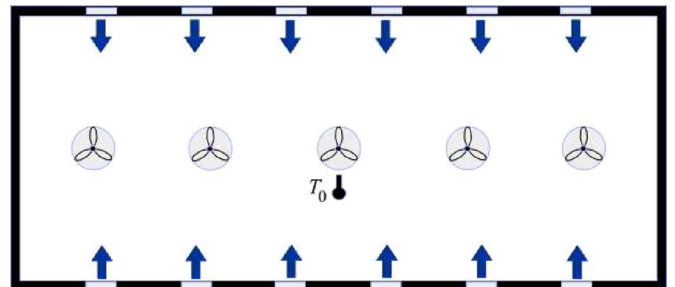


Fig. 21. Sketch of the livestock stable seen from above. The control system initially relies on one centrally placed temperature measurement, T_0 , to control the ventilation fans.

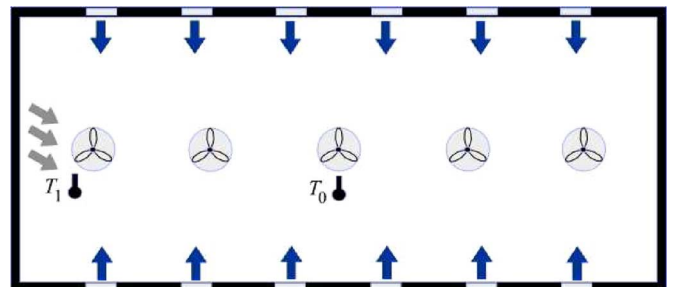


Fig. 22. Sketch of the livestock stable seen from above. The extra temperature sensor T_1 is installed to detect the leakage flow (indicated by the faded arrows to the left).

state error on both measurements, but since we have only one actuator, it is necessary to compromise. Since the temperature is lower at the new sensor, it is decided to shift the integral action to this measurement.

The factors are based on a very simple model

$$G_1 = \begin{bmatrix} G_0 \\ G_a \end{bmatrix} = \begin{bmatrix} \frac{-0.72}{1200s+1} \\ \frac{-0.88}{800s+1} \end{bmatrix}.$$

As seen from Fig. 23, this model provides a reasonably good fit.

The result of applying the method presented in Section V is shown in Fig. 24. In the beginning, K_0 is keeping T_0 at the set point. When γ is increased, the controller moves T_1 to the set point by lowering the ventilation rate.

Note that if we had wished to control the average of the two temperatures instead, this could easily have been achieved by just setting $\gamma = 1/2$.

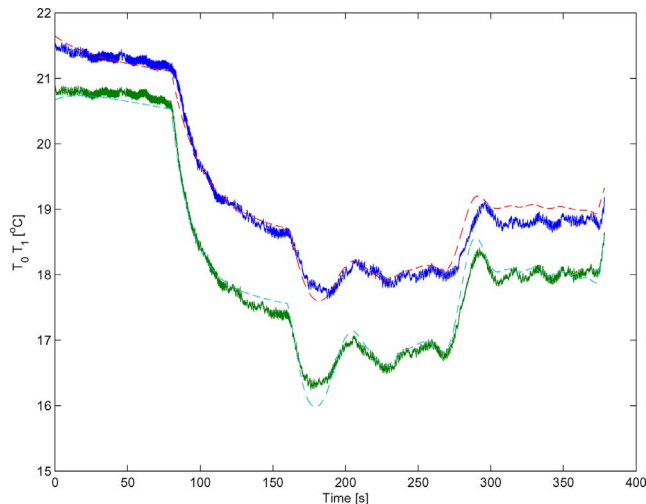


Fig. 23. Temperature measurements (solid line) from the stable compared with simple model (dashed line). A small drift term has been added to the input to compensate for the ambient temperature.

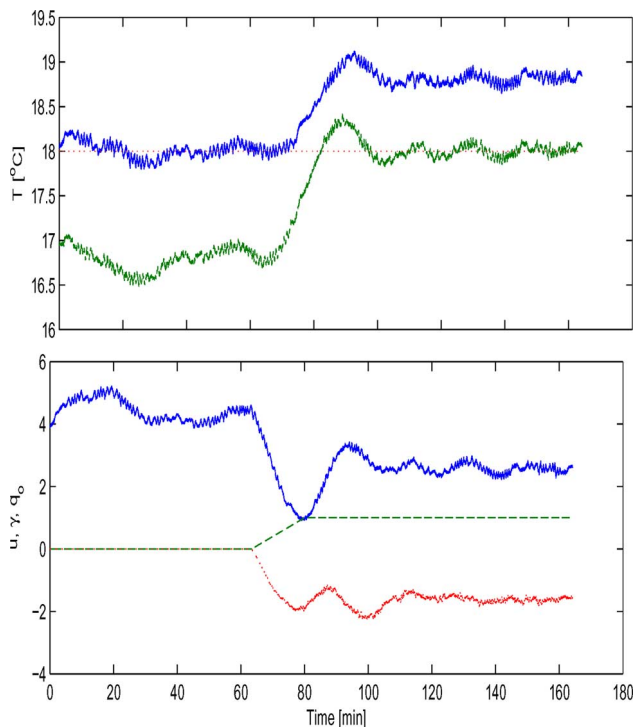


Fig. 24. Measurements from the stable. (Top plot) The two temperature measurements (blue: T_0 , green: T_1) and the reference (red, dotted line). (Bottom plot) The scheduling parameter γ (dashed line, green), the output of M (dotted line, red), and the resulting control signal (solid line, blue).

IX. CONCLUDING REMARKS

In this paper, we have considered the control aspect of “Plug-and-Play Control.” The Plug-and-Play Control problem was formulated as the problem of designing an extended controller

$K_1 = [\bar{K} \quad K_a]$ (or $K_1 = \begin{bmatrix} \bar{K} \\ K_a \end{bmatrix}$) that follows:

- utilizes a new measurement (or actuator);
- allows a *smooth transition* $K_0 \rightarrow K_1$, in the sense that the shift to the new controller should not cause large transients;

- retains closed-loop stability throughout the transition;
- allows recovering the old controller through the reverse transition $K_1 \rightarrow K_0$;

such that the performance of the closed loop is improved in some sense, e.g., by decreasing an appropriate norm.

We briefly touched upon a system identification method for identifying parameters associated with the new sensors, which often works well in closed-loop operation.

We then discussed two different approaches to incorporating new control system devices. The first approach relies on a modified Youla-Kucera parametrization of all stabilizing controllers for a given plant. We showed how the additional controller should be implemented while only accessing the terminals of the existing controller, in case the internal state of the existing controller is not available. The Youla-Kucera-based methodology has the advantage that the performance transfer function is affine in the design parameter, which means that the design problem has an open-loop-like nature and good performance can thus be expected during the transition between controllers. On the other hand, the question of actually computing the Youla-Kucera parameter in order to achieve a particular realization of a new controller in the general case remains an open problem.

The other approach presented is based on sensor fusion, in the sense that new measurements are fused with existing ones in order to modify the inputs to the existing controller, such that the overall performance is improved. A separation principle was shown to hold under mild assumptions. As with the aforementioned approach, there is still work to be done; it is not yet clear how to find the optimal weighting between new and old measurements.

Finally, we demonstrated the Plug-and-Play Control concept, as well as the practical feasibility of the proposed methods, on a laboratory-scale model of a district heating system and a live-stock stable climate system. In both cases it was possible to improve operation noticeably by exploiting new sensors and/or actuators without discarding the existing control system.

REFERENCES

- [1] A. Emami-Naeini, J. Ebert, D. De Roover, R. L. Kosut, M. Dettori, L. M. Porter, and S. Ghosal, “Modeling and control of distributed thermal systems,” *IEEE Trans. Control Syst. Technol.*, vol. 11, no. 5, pp. 668–683, Sep. 2003.
- [2] M. J. Araúzo-Bravo, J. M. Cano-Izquierdo, E. Gómez-Sánchez, M. J. López-Nieto, Y. A. Dimitriadis, and J. López-Coronado, “Automatization of a penicillin production process with soft sensors and an adaptive controller based on neuro fuzzy systems,” *Control Eng. Pract.*, vol. 12, no. 9, pp. 1073–1090, 2004.
- [3] H. Bouhenchir, M. Cabassud, and M. V. Le Lann, “Predictive functional control for the temperature control of a chemical batch reactor,” *Comput. Chem. Eng.*, vol. 30, no. 6, pp. 1141–1154, 2006.
- [4] A. G. Soldatos, K. G. Arvanitis, G. D. Pasgianos, and N. A. Sigrimis, “Nonlinear robust temperature-humidity control in livestock buildings,” *Comput. Electron. Agriculture*, vol. 49, no. 3, pp. 357–376, 2005.
- [5] F. Casella, C. Maffezzoni, L. Piroddi, and F. Pretolani, “Minimising production costs in generation and cogeneration plants,” *Control Eng. Pract.*, vol. 9, no. 3, pp. 283–295, 2001.
- [6] T. Knudsen, K. Trangbaek, and C. S. Kallešøe, “Plug and play process control applied to a district heating system,” presented at the 17th IFAC World Congr., Seoul, Korea, 2008.
- [7] A. G. Michelsen, R. Izadi-Zamanabadi, and J. Stoustrup, “Towards automatic model based controller design for reconfigurable plants,” presented at the IFAC World Congr., Seoul, Korea, 2008.

- [8] J. Bendtsen, K. Trangbaek, and J. Stoustrup, "Plug-and-play process control: Improving control performance through sensor addition and pre-filtering," presented at the 17th IFAC World Congr., Seoul, Korea, 2008.
- [9] M. E. Hangstrup, J. Stoustrup, P. Andersen, and T. S. Pedersen, "Gain-scheduled control of a fossil-fired power plant boiler," in *Proc. IEEE Int. Conf. Control Appl.*, 1999, pp. 905–909.
- [10] M. Rotkowitz and S. Lall, "A characterization of convex problems in decentralized control," *IEEE Trans. Autom. Control*, vol. 50, no. 12, pp. 1984–1996, Dec. 2005.
- [11] C. Khambampati, R. J. Patton, A. Casavola, and G. Franze, "Fault-tolerance as a key requirement for the control of modern systems," in *Proc. 6th IFAC Symp. Fault Detection, Supervision, Safety Techn. Processes*, 2006, pp. 26–36.
- [12] R. J. Patton, C. Khambampati, and F. J. Uppal, "Reconfiguration in networked control systems: Fault tolerant control and plug-and-play," in *Proc. 6th IFAC Symp. Fault Detection, Supervision, Safety Techn. Processes*, 2006, pp. 151–156.
- [13] A. Rantzer, "On prize mechanisms in linear quadratic team theory," in *Proc. IEEE Conf. Decision Control*, 2007, pp. 1112–1116.
- [14] W. S. Lee, B. D. O. Anderson, I. M. Y. Mareels, and R. L. Kosut, "On some key issues in the windsurfer approach to adaptive robust control," *Automatica*, vol. 31, no. 11, pp. 1619–1636, 1995.
- [15] B. D. O. Anderson, T. Brinsmead, D. Liberzon, and S. Morse, "Multiple model adaptive control with safe switching," *Int. J. Adapt. Control Signal Process.*, vol. 15, pp. 445–470, 2001.
- [16] A. Dehghani, B. D. O. Anderson, and A. Lanzon, "An H_∞ algorithm for the windsurfer approach to adaptive robust control," *Int. J. Adapt. Control Signal Process.*, vol. 18, pp. 607–628, 2004.
- [17] T. Knudsen, "Incremental data driven modelling for plug and play process control," presented at the 47th IEEE Conf. Decision Control, Budapest, Hungary, 2008.
- [18] F. Hansen, G. Franklin, and R. Kosut, "Closed-loop identification via the fractional representation: Experiment design," presented at the Amer. Control Conf., Pittsburgh, PA, 1989.
- [19] B. D. O. Anderson, "From Youla-Kucera to identification, adaptive and nonlinear control," *Automatica*, vol. 34, pp. 1485–1506, 1998.
- [20] B. V. Dasarthy, *Decision Fusion*. New York: IEEE Press, 1994.
- [21] R. R. Brooks and S. S. Iyengar, *Multiple-Sensor Fusion—Fundamentals and Applications with Software*. Englewood Cliffs, NJ: Prentice-Hall, 1998.
- [22] M. Abdelrahman and P. Kandasamy, "Integration of multiple sensor fusion in controller design," *ISA Trans.*, vol. 42, pp. 197–205, 2003.
- [23] D. C. Youla, H. A. Jabr, and J. J. Bongiorno, "Modern Wiener-Hopf design of optimal controllers – Part II: The multivariable case," *IEEE Trans. Autom. Control*, vol. 21, no. 3, pp. 319–338, 1976.
- [24] V. Kucera, "Stability of discrete linear feedback systems," presented at the 6th IFAC World Congr., Boston, MA, 1976.
- [25] H. Niemann, "Parameterisation of extended systems," *IEE Proc.: Control Theory Appl.*, vol. 153, pp. 221–227, 2006.
- [26] K. Zhou, J. C. Doyle, and K. Glover, *Robust and Optimal Control*. Englewood Cliffs, NJ: Prentice-Hall, 1996.
- [27] J. Stoustrup and H. Niemann, "Multiple model adaptive control with safe switching," in *Proc. Amer. Control Conf.*, 1999, pp. 4029–4033.
- [28] H. Niemann, J. Stoustrup, and R. B. Abrahamsen, "Switching between multivariable controllers," *Optimal Control Appl. Methods*, vol. 25, pp. 51–66, 2004.
- [29] J. Bendtsen, J. Stoustrup, and K. Trangbaek, "Bumpless transfer between observer-based gain scheduled controllers," *Int. J. Control*, vol. 78, no. 7, pp. 491–504, 2005.
- [30] B. A. Francis, *A Course in H-infinity Control Theory*, M. Thoma and A. Wyner, Eds. New York: Springer-Verlag, 1987, vol. 88, Lecture Notes in Control and Information Sciences.
- [31] J. Bendtsen, K. Trangbaek, and J. Stoustrup, "Closed-loop system identification with new sensors," presented at the 47th IEEE Conf. Decision Control, Cancun, Mexico, 2008.
- [32] G. Vinnicombe, *Uncertainty and Feedback*. London, U.K.: Imperial College Press, 2001.
- [33] K. Trangbaek, J. Stoustrup, and J. Bendtsen, "Stable controller reconfiguration through terminal connections," presented at the IFAC World Congr., Seoul, Korea, 2008.
- [34] J. Stoustrup, "Plug & play control: Control technology towards new challenges," *Euro. J. Control*, vol. 15, no. 4, pp. 311–330, 2009.
- [35] K. Trangbaek, T. Knudsen, and C. S. Kallesoe, "Plug and play process control of a district heating system," presented at the Euro. Control Conf., Budapest, Hungary, 2009.
- [36] K. Trangbaek and J. Bendtsen, "Stable controller reconfiguration through terminal connections – A practical example," presented at the 7th IEEE Int. Conf. Control Autom., Christchurch, New Zealand, 2009.



Jan Bendtsen (M'11) was born in Rodovre, Denmark, in 1972. He received the M.Sc. degree in electrical engineering and the Ph.D. degree in control engineering from the Department of Control Engineering, Aalborg University, Aalborg, Denmark, in 1996 and 1999, respectively.

Since 1999, he has been an Assistant Professor and subsequently Associate Professor with the Department of Electronic Systems, Automation and Control, Aalborg University. During the Winter of 2005, he was Visiting Scholar with NICTA, Australian National University. Since 2006, he has been work package manager of several large research projects and has been on several organizing committees for international conferences as well. His research interests include adaptive control of nonlinear systems, closed loop system identification, control of energy systems and linear parameter varying systems.

Prof. Bendtsen was a co-recipient of the Best Technical Paper Award at the AIAA Guidance, Navigation, and Control Conference, 2009.



Klaus Trangbaek was born in Aarhus, Denmark, in 1973. He received the M.Sc. and Ph.D. degrees from the Department of Electronic Systems, Automation, and Control, Aalborg University, Aalborg, Denmark, in 1997 and 2001, respectively.

From 2001 to 2003, he worked with controller development for Grundfos A/S, Bjerringbro, Denmark. From 2003 to 2011, he was an Assistant and then an Associate Professor with Aalborg University. His research interests include controller modification, closed-loop system identification, smart grids and

linear parameter varying systems.



Jakob Stoustrup (SM'99) received the M.Sc. degree in electrical engineering and the Ph.D. degree in applied mathematics from the Department of Mathematics, Technical University of Denmark, Lyngby, Denmark, in 1987 and 1991, respectively.

He held several positions at the Technical University of Denmark, including Visiting Professorships at the University of Strathclyde, Glasgow, U.K., and the Mittag-Leffler Institute, Stockholm, Sweden. Since 1997, he was a Professor with the Department of Automation and Control, Aalborg University, Aalborg,

Denmark, and since 2006, he was Head of Research for the Department of Electronic Systems. His main contributions have been robust control, fault tolerant control, and plug-and-play control, with 200+ peer-reviewed papers. He has carried out industrial applications in cooperation with 60+ companies.

He was an Associate Editor, Guest Editor, and Editorial Board Member of several international journals. He is a past Chairman of IEEE CSS/RAS Joint Chapter. Since 2008, he was a Chairman for the IFAC Technical Committee SAFEPROCESS. Since 2011, he was a member of IFAC Technical Board, member of the Danish and Swedish Research Councils, and of The Danish Academy of Technical Sciences.